
Proceedings Paper:
Bagheri, A, Sofotasios, PC, Tsiftsis, TA et al. (2015) Area under ROC curve of energy detection over generalized fading channels. In: IEEE International Symposium on Personal, Indoor and Mobile Radio Communications, PIMRC 2015. 26th IEEE Annual International Symposium on Personal, Indoor, and Mobile Radio Communications, PIMRC 2015, 30 Aug - 02 Sep 2015, Hong Kong, China. IEEE, pp. 656-661. ISBN: 9781467367820.

https://doi.org/10.1109/PIMRC.2015.7343380

Area under ROC Curve of Energy Detection over Generalized Fading Channels

Alireza Bagheri[1], Paschalis C. Sofotasios[2,3], Theodoros A. Tsiftsis[4], Ali Shahzadi[1], Steven Freear[5], and Mikko Valkama[2]

[1]Department of Electrical and Computer Engineering, Semnan University, 35131-19111 Semnan, Iran.
Email: a_bagheri@students.semnan.ac.ir; a_shahzadi@sun.semnan.ac.ir
[2]Department of Electronics and Communications Engineering, Tampere University of Technology, 33101 Tampere, Finland.
Email: {paschalis.sofotasios;mikko.e.valkama}@tut.fi
[3]Department of Electrical and Computer Engineering, Aristotle University of Thessaloniki, 54636 Thessaloniki, Greece.
[4]Department of Electrical Engineering, Technological Educational Institute of Central Greece, 35100 Lamia, Greece.
Email: tsiftsis@teilam.gr
[5]School of Electronic and Electrical Engineering, University of Leeds, LS2 9JT Leeds, UK.
Email: s.freear@leeds.ac.uk

***Abstract*—A fast and reliable detection scheme is essential in several wireless applications such as radar and cognitive radio systems. Energy detection is such a method as it does not require a priori information of the received signal while it exhibits low implementation complexity and costs. Since the detection capability of ED is largely affected by the effects of multipath fading, this paper is devoted to a thorough analysis of energy detection based spectrum sensing over generalized fading conditions. To this end, analytical expressions are firstly derived using the area under the receiver operating characteristic curve (AUC) under additive white Gaussian noise. This analysis is subsequently extended to the case of generalized fading conditions characterized by $\kappa-\mu$ and $\eta-\mu$ fading distributions. The offered results are novel and are employed in analyzing the corresponding performance. It is shown that fading phenomena result to detrimental effects on the performance of spectrum sensing since the deviation between severe and non-severe conditions is rather substantial.**

I. Introduction

Signal detection is the basic and essential mechanism in numerous wireless applications and has for long attracted significant interest by both academic and industrial sectors. For instance, realization of a cognitive radio system, as an intelligent radio that can sense and exploit the spectral gaps, has become a notable topic of research over the past decade. Among various detection schemes such as matched filter, cyclostationary or feature detection, energy detection (ED) has been considered a simple and efficient detection method [2], [3] as its blind (non-coherent) structure does not require any prior knowledge about the signal under test (SUT) [4]–[7].

Detection performance of the ED based sensing method is classically characterized by two key measurement metrics: probability of detection (P_d) and probability of false alarm (P_{fa}). The receiver operating characteristics (ROC) curve, P_d versus P_{fa}, can be used to illustrate and quantify the detection capability of energy detectors. By also recalling that information signals are largely distorted by fading phenomena [8]–[21], the performance of detection methods is also largely affected when the SUT is dominated by multipath fading and time varying conditions of channels. Based on this, several studies have been devoted to the analysis of ED based sensing over different fading channels in terms of the ROC curves, e.g. see [22]–[29], and the references therein. However, although the ROC curves can provide an adequate indication of ED performance, it is a relatively restrictive approach as it holds only for specific values of P_{fa}. Hence, a single figure of merit that provides a better insight on the overall detection performance is undoubtedly useful. To this end, a single-parameter measure that has been used widely in applications relating to natural sciences and engineering is the area under the ROC curve (AUC) [30]. The value of AUC varies between 0.5 and 1, with values between 0.8 and 1 denoting acceptable detection performance [30]–[33]. The distinct characteristic of AUC is that when its value is unity, the performance of the detector is perfect not only for specific values. This is in fact the limitation of the ROC curves since any determined probability of detection is valid for specific P_{fa} values; the reason is that AUC is fundamentally based on prior averaging over all values of P_{fa}. This measure was firstly introduced in the context of wireless communications in, see e.g. [30], [34]. Based on this, the authors in [35] analyzed the AUC by means of the semi-analytic MGF approach for the case of Nakagami$-m$ and $\eta-\mu$ fading channels while similar analyses based on the MGF approach were reported in [36], [37].

It is also recalled that the $\kappa-\mu$ and $\eta-\mu$ distributions are generic fading models which have been recently proposed in [38] to provide a better modeling of small-scale variations of the fading signal in line-of-sight (LOS) and non-line-of-sight (NLOS) conditions, respectively. Furthermore, the $\kappa-\mu$ distribution includes the Rice (Nakagami-n) and the Nakagami-m distributions, while the $\eta-\mu$ distribution comprises both the Hoyt and the Nakagami-m as, special cases [38]. Motivated by this, the present work is devoted to the analysis of AUC based energy detection over generalized fading channels. To this end and unlike most reported analyses, novel closed-form expressions are derived for arbitrary values of the time-bandwidth product, u in terms of the generalized Lauricella hypergeometric functions and they are subsequently employed in analyzing the ED performance over various fading scenarios. As expected, the detection behaviour of the ED is highly dependent upon the value and variations of the involved fading

parameters. This allows accurate quantification of the effect of fading on the system performance for various scenarios which can enable the determination of the required power levels for ensuring robust and efficient performance of energy detectors.

II. Preliminaries

A. System Model and Detection

The problem of detecting the presence of unknown wireless signals can be modeled as a binary hypothesis-testing problem, where hypotheses H_0 and H_1 correspond to the cases when the SUT is absent or present, respectively. The received signal for the binary hypothesis can be given as

$$y(t) = \begin{cases} n(t) & : H_0 \\ hx(t) + n(t) & : H_1 \end{cases} \quad (1)$$

where h and $n(t)$ denote the wireless channel gain and zero-mean complex additive white Gaussian noise (AWGN) with single-sided power spectral density N_0 at the receiver, respectively, and $x(t)$ is the transmitted signal with average power E_x. Based on this, the received signal is firstly filtered with a band-pass filter in bandwidth $W(\text{Hz})$ to remove the noise and adjacent interference. Then, the output of this filter is squared and integrated over time duration T to produce the test statistic Y which can be represented as [23]

$$Y \sim \begin{cases} \chi^2_{2u} & : H_0 \\ \chi^2_{2u}(2\gamma) & : H_1 \end{cases} \quad (2)$$

where χ^2_{2u} denotes a central chi-square distribution with $2u$ degrees of freedom, where u is the time-bandwidth product. Furthermore, $\chi^2_{2u}(2\gamma)$ is a non-central chi-square distribution with the same degrees of freedom and a non-centrality parameter 2γ, where γ ($\gamma \geq 0$) is the received instantaneous SNR of the target signal given as $\gamma = |h|^2 E_x/N_0$. Finally, the test statistic Y is compared to a predefined threshold λ to determine the absence or presence of the SUT. In the AWGN case, where the channel gain h is deterministic, the probabilities of false alarm (P_{fa}) and detection (P_d) are given by [23]

$$P_{fa} = \Pr(Y > \lambda | H_0) = Q\left(u, \frac{\lambda}{2}\right) \quad (3)$$

and

$$P_d = \Pr(Y > \lambda | H_1) = Q_u\left(\sqrt{2\gamma}, \sqrt{\lambda}\right) \quad (4)$$

where $Q(.,.)$ is the regularized Gamma function and $Q_u(a,b)$ is the generalized Marcum Q-function [39].

B. Generalized Fading Channels

1) The $\kappa-\mu$ Distribution: The $\kappa-\mu$ fading model considers a signal composed of clusters of multipath waves, propagating in a non-homogeneous environment. The clusters of multipath waves are assumed to have scattered waves with identical powers, but each cluster includes a dominant component, which presents an arbitrary power [38]. The parameter κ denotes the ratio between the total power of the dominant components and the total power of the scattered waves, whereas the parameter μ is related to the number of multipath clusters. The corresponding PDF of the instantaneous SNR per symbol, γ, is given by [38, eq. (10)], namely

$$f_\gamma(\gamma) = \frac{\mu(1+\kappa)^{\frac{\mu+1}{2}}}{\kappa^{\frac{\mu-1}{2}}\exp(\kappa\mu)} \frac{\gamma^{\frac{\mu-1}{2}} I_{\mu-1}\left(2\mu\sqrt{\frac{\kappa(1+\kappa)\gamma}{\bar{\gamma}}}\right)}{\bar{\gamma}^{\frac{\mu+1}{2}}\exp\left(\frac{\mu(1+\kappa)\gamma}{\bar{\gamma}}\right)} \quad (5)$$

where $\bar{\gamma}$ represents the average SNR per symbol, and $I_n(.)$ is the n^{th} order modified Bessel function of the first kind [40]. Notably, the $\kappa-\mu$ distribution includes as special case the Rice distribution for $\mu = 1$, the Nakagami$-m$ distribution for $\kappa \to 0$, the Rayleigh distribution for $\mu = 1$ and $\kappa \to 0$ and the One-Sided Gaussian for $\mu = 0.5$ and $\kappa \to 0$, [38].

2) The $\eta-\mu$ Distribution: The physical interpretation of the $\eta-\mu$ fading distribution is based on considering a signal composed of clusters of multipath waves propagating in a non-homogeneous environment. This model consists of two formats with μ denoting the number of multipath clusters [38]. In Format I, $0 < \eta < \infty$ denotes the ratio between the in-phase and quadrature components of the signal in each cluster. These components are assumed to be statistically independent to each other and have different powers. In Format II, $-1 < \eta < 1$ denotes the correlation between the powers of the in-phase and quadrature scattered waves in each multipath cluster.

The $\eta-\mu$ SNR distribution is expressed as [38, eq. (26)]

$$f_\gamma(\gamma) = \frac{2\sqrt{\pi}h^\mu \mu^{\mu+\frac{1}{2}} \gamma^{\mu-\frac{1}{2}} I_{\mu-1}\left(\frac{2\mu H}{\bar{\gamma}}\gamma\right)}{\Gamma(\mu) H^{\mu-\frac{1}{2}} \bar{\gamma}^{\mu+\frac{1}{2}} \exp\left(\frac{2\mu h}{\bar{\gamma}}\gamma\right)} \quad (6)$$

where $h = \left(2 + \eta^{-1} + \eta\right)/4$, $H = \left(\eta^{-1} - \eta\right)/4$, in Format I and $h = 1/\left(1-\eta^2\right)$, $H = \eta/\left(1-\eta^2\right)$ in Format II. It is also recalled that the $\eta-\mu$ distribution reduces to Nakagami$-q$ (Hoyt) distribution for $\mu = 0.5$ and to Nakagami$-m$ distribution for $\eta \to 0, \eta \to \infty$, and $\eta \to \pm 1$, [38].

III. Area Under ROC Curve (AUC) Analysis

Closed-form expressions are derived for the average AUC over generalized fading channels. To this end, it is firstly essential to derive an exact closed-form expression for the AUC under AWGN for arbitrary values of u that can act as a benchmark for all future analyses in cognitive radio systems.

A. The AUC under Non-Fading Channels

The AUC is the area covered by the ROC curve of P_d versus P_f and is defined as [30]

$$A = \int_0^1 P_d(\gamma, \lambda)\, \mathrm{d}P_{fa}(\lambda). \quad (7)$$

Based on this, the average AUC ($\overline{\text{AUC}}$) under different fading conditions is determined as follows

$$\overline{\text{AUC}} = \int_0^\infty A(\gamma) f_\gamma(\gamma)\, \mathrm{d}\gamma. \quad (8)$$

It is recalled that the AUC under AWGN for the case of arbitrary values of u is given by [36, eq. (8)], namely

$$A(\gamma) = \sum_{l=0}^{\infty} \frac{(l+u)_u \gamma^l}{l! 2^{l+2u} e^\gamma} {}_2\tilde{F}_1\left(1, l+2u; 1+u; \frac{1}{2}\right) \quad (9)$$

where $(x)_n$ and ${}_2\tilde{F}_1(\cdot,\cdot;\cdot;\cdot)$ denote the Pochhammer symbol, and the regularized confluent hypergeometric function, respectively [41]. hence. by expanding the above series one obtains

$$A(\gamma)=\sum_{l=0}^{\infty}\sum_{i=0}^{\infty}\frac{(l+u)_u(1)_i(l+2u)_i}{l!2^{l+2u}(1+u)_i\Gamma(1+u)}\gamma^l e^{-\gamma} \tag{10}$$

and by recalling the standard Pochhammer symbol identities along with the Legendre duplication formula yields

$$A(\gamma)=\frac{\Gamma\left(u+\frac{1}{2}\right)}{2u!\sqrt{\pi}e^{\gamma}}\sum_{l=0}^{\infty}\sum_{i=0}^{\infty}\frac{(2u)_{l+i}(1)_l}{(1+u)_l(u)_i}\frac{1}{l!2^l}\frac{\gamma^i}{i!2^i}. \tag{11}$$

Importantly, for $\gamma,u\in\mathbb{R}^+$, the following closed-form expressions are deduced for the AUC under AWGN case:

$$A(\gamma)=\frac{\Gamma\left(u+\frac{1}{2}\right)\Psi_1\left(2u,1,1+u,u;\frac{1}{2},\frac{\gamma}{2}\right)}{2u!\sqrt{\pi}e^{\gamma}} \tag{12}$$

$$=\frac{\Gamma\left(u+\frac{1}{2}\right)F_2\left(2u,1,-,1+u,u;\frac{1}{2},\frac{\gamma}{2}\right)}{2u!\sqrt{\pi}e^{\gamma}} \tag{13}$$

where $\Psi_1(.)$ and $F_2(.)$ denote the Humbert and Appell special functions, respectively [41].

B. Average AUC over $\kappa-\mu$ Fading Channels

The average AUC over $\kappa-\mu$ fading channels when $u\in\mathbb{R}^+$ can be evaluated by substituting (5) in (8) yielding

$$\overline{\mathrm{AUC}}=\frac{e^{-\kappa\mu}\zeta^{\frac{\mu+1}{2}}}{(\kappa\mu)^{\frac{\mu-1}{2}}}\sum_{l=0}^{\infty}\frac{(l+u)_u}{l!2^{l+2u}}{}_2\tilde{F}_1\left(1,l+2u;1+u;\frac{1}{2}\right)\times\underbrace{\int_0^{\infty}\gamma^{\frac{\mu-1}{2}+l}e^{-(1+\zeta)\gamma}I_{\mu-1}\left(2\sqrt{\kappa\mu\zeta\gamma}\right)\mathrm{d}\gamma}_{\mathcal{I}_1} \tag{14}$$

where $\zeta=\mu(1+\kappa)/\bar{\gamma}$. Notably, the above integral is identical to [40, eq. (6.643.2)] and thus, it can be expressed in terms as

$$\mathcal{I}_1=\frac{(\mu)_l}{\sqrt{\kappa\mu\zeta}}\left(\frac{1}{1+\zeta}\right)^{l+\frac{\mu}{2}}e^{\frac{\kappa\mu\zeta}{2(1+\zeta)}}M_{-\left(l+\frac{\mu}{2}\right),\frac{\mu-1}{2}}\left(\frac{\kappa\mu\zeta}{1+\zeta}\right). \tag{15}$$

Also, with the aid of [40, eq. (9.220.2)], it follows that

$$\mathcal{I}_1=\frac{(\mu)_l(\kappa\mu\zeta)^{\frac{\mu-1}{2}}}{(1+\zeta)^{l+\mu}}{}_1F_1\left(\mu+l;\mu;\frac{\kappa\mu\zeta}{1+\zeta}\right) \tag{16}$$

where ${}_1F_1(.,.;.)$ is the Kummer's confluent hypergeometric function [41]. Thus, by substituting (16) into (14) one obtains

$$\overline{\mathrm{AUC}}=\sum_{l=0}^{\infty}\frac{\zeta^{\mu}e^{-\kappa\mu}\Gamma(l+\mu)\Gamma(l+2u)}{4^u\Gamma(l+u)\,l!2^l(1+\zeta)^{\mu+l}}\times{}_2\tilde{F}_1\left(1,l+2u;1+u;\frac{1}{2}\right){}_1\tilde{F}_1\left(\mu+l;\mu;\frac{\kappa\mu\zeta}{1+\zeta}\right). \tag{17}$$

Expanding the regularized confluent hypergeometric functions, expressing each gamma function in terms of the Pochhammer function, using the Legendre duplication formula and u carrying out long but basic algebraic manipulations yields

$$\overline{\mathrm{AUC}}=\sum_{l=0}^{\infty}\sum_{i=0}^{\infty}\sum_{j=0}^{\infty}\frac{(2u)_{l+i}(\mu)_{l+j}(1)_i}{(u)_l(1+u)_i(\mu)_j}\frac{\left(\frac{1}{2(1+\zeta)}\right)^l}{c_1^{-1}l!}\frac{\left(\frac{1}{2}\right)^i}{i!}\frac{\left(\frac{\kappa\mu\zeta}{1+\zeta}\right)^j}{j!} \tag{18}$$

where

$$c_1=\frac{e^{-\kappa\mu}\Gamma\left(u+\frac{1}{2}\right)}{2\sqrt{\pi}\Gamma(u+1)}\left(\frac{\zeta}{1+\zeta}\right)^{\mu}. \tag{19}$$

To this effect, the average AUC over $\kappa-\mu$ fading channels can be computed in closed-form according to (20), at the top of the next page, where $F_{C:D';\ldots;D^{(n)}}^{A:B';\ldots;B^{(n)}}$ denotes the Lauricella hypergeometric function in n variables [42].

C. The Average AUC under $\eta-\mu$ Fading Channels

By averaging (9) over the fading statistics in (6) one obtains

$$\overline{\mathrm{AUC}}=\sum_{l=0}^{\infty}\frac{2\sqrt{\pi H}\mu^{\mu+\frac{1}{2}}h^{\mu}(l+u)_u}{\Gamma(\mu)H^{\mu}l!2^{l+2u}\bar{\gamma}^{\mu+\frac{1}{2}}}{}_2\tilde{F}_1\left(1,l+2u;1+u;\frac{1}{2}\right)\times\underbrace{\int_0^{\infty}\gamma^{\mu+l-\frac{1}{2}}e^{-\left(1+\frac{2\mu h}{\bar{\gamma}}\right)\gamma}I_{\mu-\frac{1}{2}}\left(\frac{2\mu H}{\bar{\gamma}}\gamma\right)\mathrm{d}\gamma}_{\mathcal{I}_2}. \tag{21}$$

By also utilizing [43, eq. (03.02.06.0038.01)] and [40, eq. (7.525.1)], it follows that

$$\mathcal{I}_2=\frac{\left(\frac{\mu H}{\bar{\gamma}}\right)^{\mu-\frac{1}{2}}\Gamma(l+2\mu)}{\left(1+\frac{2\mu h}{\bar{\gamma}}\right)^{l+2\mu}}\times{}_2\tilde{F}_1\left(\frac{l+2\mu}{2},\frac{l+2\mu+1}{2};\frac{2\mu+1}{2};\left(\frac{2\mu H}{\bar{\gamma}+2\mu h}\right)^2\right). \tag{22}$$

By substituting $\mathcal{I}_2$ in (21) and expanding the involved hypergeometric functions one obtains

$$\overline{\mathrm{AUC}}=\frac{\sqrt{\pi}}{2^{2u-1}}\left(\frac{\mu\sqrt{h}}{\bar{\gamma}+2\mu h}\right)^{2\mu}\frac{\Gamma(2u)\Gamma(2\mu)}{\Gamma(u)\Gamma(1+u)\Gamma(\mu)\Gamma\left(\mu+\frac{1}{2}\right)} \tag{23}$$

$$\times\sum_{l=0}^{\infty}\sum_{i=0}^{\infty}\sum_{j=0}^{\infty}\frac{2^{2j-i-l}\bar{\gamma}^l(\mu H)^{2j}(2u)_{l+i}(\mu)_{\frac{l}{2}+j}\left(\mu+\frac{1}{2}\right)_{\frac{l}{2}+j}(2\mu)_l}{l!j!(\bar{\gamma}+2\mu h)^{l+2j}(u)_l(\mu)_{\frac{l}{2}}\left(\mu+\frac{1}{2}\right)_{\frac{l}{2}}(1+u)_i\left(\mu+\frac{1}{2}\right)_j}.$$

With the aid of the Pochhammer symbol identity $(x)_{2n}=2^{2n}(\frac{x}{2})_n(\frac{x+1}{2})_n$, it follows that $(2\mu)_l=2^l(\mu)_{\frac{l}{2}}(\mu+\frac{1}{2})_{\frac{l}{2}}$ and $(\mu)_{\frac{l}{2}+j}(\mu+\frac{1}{2})_{\frac{l}{2}+j}=2^{-(l+2j)}(2\mu)_{l+2j}$. Thus, (23) becomes

$$\overline{\mathrm{AUC}}=\frac{\sqrt{\pi}}{2^{2u-1}}\left(\frac{\mu\sqrt{h}}{\bar{\gamma}+2\mu h}\right)^{2\mu}\frac{\Gamma(2u)\Gamma(2\mu)}{\Gamma(u)\Gamma(1+u)\Gamma(\mu)\Gamma\left(\mu+\frac{1}{2}\right)} \tag{24}$$

$$\times\sum_{l=0}^{\infty}\sum_{i=0}^{\infty}\sum_{j=0}^{\infty}\frac{(2\mu)_{l+2j}(2u)_{l+i}(1)_i}{(u)_l(1+u)_i\left(\mu+\frac{1}{2}\right)_j}\frac{\left(\frac{\bar{\gamma}}{2(\bar{\gamma}+2\mu h)}\right)^l}{l!}\frac{\left(\frac{1}{2}\right)^i}{i!}\frac{\left(\frac{\mu H}{\bar{\gamma}+2\mu h}\right)^{2j}}{j!}.$$

Based on this and after basic algebraic manipulations the average AUC over $\eta-\mu$ fading channels for $\bar{\gamma},\mu,h,H,u\in\mathbb{R}^+$ can be expressed in closed-form as in (26) given at the top of the next page, where $X_{17}(\cdot)$ denotes the Exton function and

$$c_2=\frac{(2\mu\sqrt{h})^{2\mu}}{2u(\bar{\gamma}+2\mu h)^{2\mu}B(u,1/2)} \tag{25}$$

with $B(\cdot,\cdot)$ denoting the Beta function [44].

$$\overline{\mathrm{AUC}}_{u\in\mathbb{R}^+}^{\kappa-\mu} = c_1 F_{0:1;1;1}^{2:0;0;1}\left[\begin{matrix}(2u:1,0,1),(\mu:1,1,0):-;-;(1:1)\\ -:(u:1);(\mu:1);(1+u:1)\end{matrix}\middle|\frac{1}{2(1+\zeta)},\frac{\kappa\mu\zeta}{1+\zeta},\frac{1}{2}\right] \tag{20}$$

$$\overline{\mathrm{AUC}}_{u\in\mathbb{R}^+}^{\eta-\mu} = c_2 X_{17}\left(2\mu,2u,1;u,1+u,\mu+\frac{1}{2};\frac{\bar{\gamma}}{2\left(\bar{\gamma}+2\mu h\right)},\frac{1}{2},\frac{\mu^2H^2}{(\overline{\gamma}+2\mu h)^2}\right) \tag{26}$$

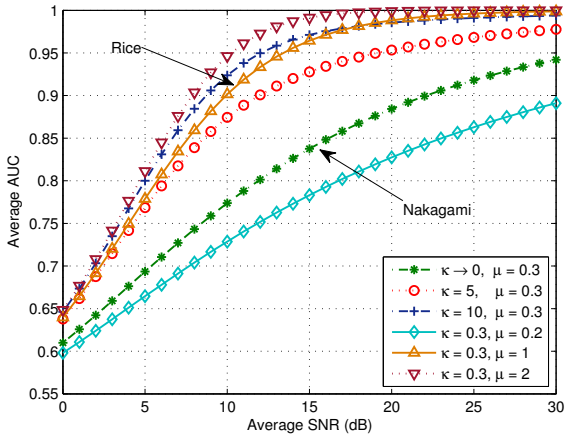

Fig. 1. Average AUC versus average SNR for $\kappa-\mu$ fading channels with $u = 2$, and different values of κ and μ.

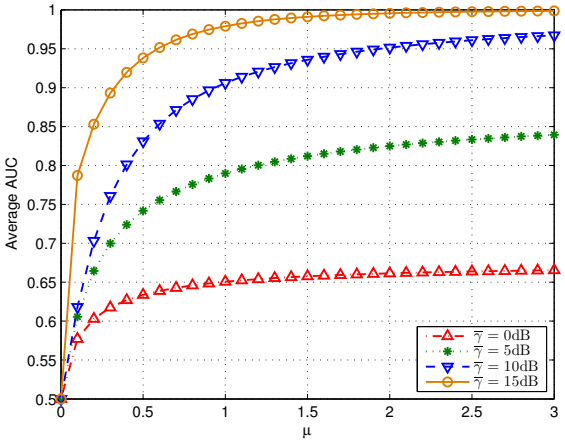

Fig. 3. Average AUC versus μ for $\kappa-\mu$ fading with $u = 1.5$, $\kappa = 0.1$, and different values of $\overline{\gamma}$.

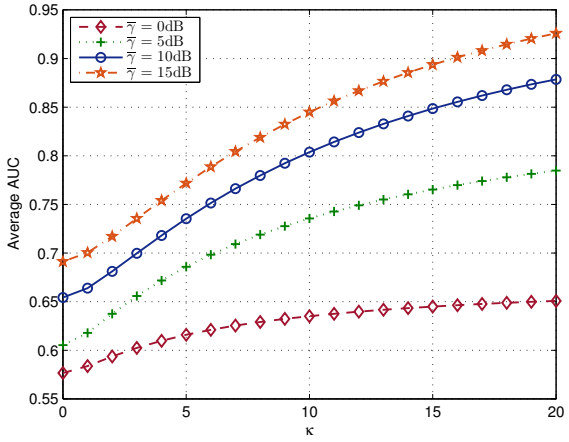

Fig. 2. Average AUC versus κ for $\kappa-\mu$ fading with $u = 1.5$, $\mu = 0.1$, and different values of $\overline{\gamma}$.

IV. Numerical Results

This Section is devoted to the analysis of the behavior of ED over $\kappa-\mu$ and $\eta-\mu$ fading channels. The corresponding performance is evaluated for different scenarios of interest through $\overline{A}$ versus $\overline{\gamma}$ curves. In addition, the effect of the fading parameters κ, η, and μ on the value of AUC is numerically quantified. To this end, Fig. 1 presents the AUC curves for the $\kappa-\mu$ fading channel model for different κ and μ values with $u = 2$. As can be seen, the energy detector shows better detection capability for both larger values of κ and μ. This is because the detector shows better detection capability for higher κ (with fixed μ) because the receiver receives more power through dominant components. On the contrary, μ plays a more important role in determining the detection performance due to the non-negligible effects of multipath fading. For example, for the case of $\overline{\gamma} = 10$dB and $\mu = 0.3$ (fixed), the $\overline{A}$ for $\kappa = 10$ is 5.6% higher than for the case of $\kappa = 5$. Likewise, when $\kappa = 0.3$ (fixed), the $\overline{A}$ for $\mu = 2$ is nearly 5% higher than for $\mu = 1$. In Fig. 1, the case in which $\kappa \to 0$ ($\mu = 0.3$) coincides with that for Nakagami-m with $m = 0.3$, where m is the Nakagami parameter. In addition, the case that $\kappa = 0.3$ ($\mu = 1$) coincides with that for Rice with $K = 0.3$, where K is the Rice parameter, or equivalently with that of Nakagami-n with $n^2 = 0.3$.

It is also important to quantify the effect of the fading parameters on the system performance explicitly. To this end, Fig. 2 presents the behavior of $\overline{A}$ versus κ for $u = 1.5$, $\mu = 0.1$, and different values of $\overline{\gamma}$. One can observe the significant deviation of $\overline{A}$ even for small variations of κ and/or $\overline{\gamma}$. Clearly, for $\overline{\gamma} = 5$dB, it is shown that $\overline{A} = 0.67$ and $\overline{A} = 0.72$ for $\kappa = 4$ and $\kappa = 8$, respectively. In addition, for $\kappa = 12$, one obtains $\overline{A} = 0.75$ for $\overline{\gamma} = 5$dB, and $\overline{A} = 0.82$ for $\overline{\gamma} = 10$dB. Likewise, the behaviour of $\overline{A}$ versus μ is shown in Fig. 3 for $u = 1.5$, $\kappa = 0.1$, and different values of $\overline{\gamma}$. It is clearly shown that the $\overline{A}$ is very sensitive as even slight variations of μ change its value rapidly. For example, for $\overline{\gamma} = 5$dB, it is shown that $\overline{A} = 0.66$ and $\overline{A} = 0.72$ for $\mu = 0.2$ and $\mu = 0.4$, respectively. Furthermore, for $\mu = 1.5$, $\overline{A} = 0.81$ for $\overline{\gamma} = 5$dB, and $\overline{A} = 0.94$ for $\overline{\gamma} = 10$dB. On a basis of comparing the two fading parameters on detection capability of the energy detector, it is evident that the effect of κ is significant for its larger values and the impact of μ is

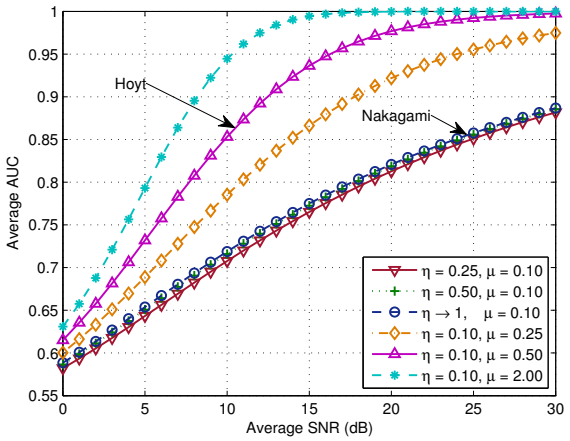

Fig. 4. Average AUC versus average SNR for $\eta-\mu$ fading channels with $u = 3$, and different values of η and μ.

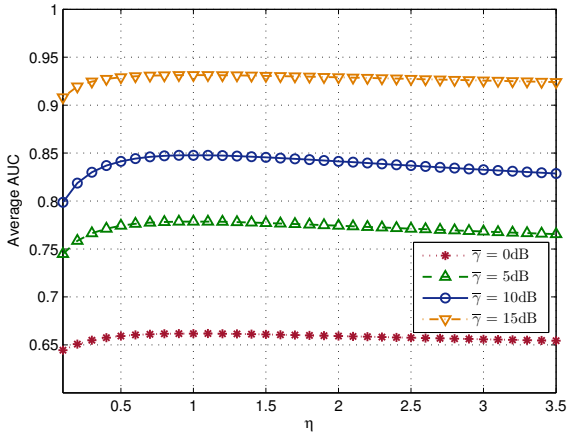

Fig. 5. Average AUC versus η for $\eta-\mu$ fading with $u = 0.75$, $\mu = 0.3$, and different values of $\overline{\gamma}$.

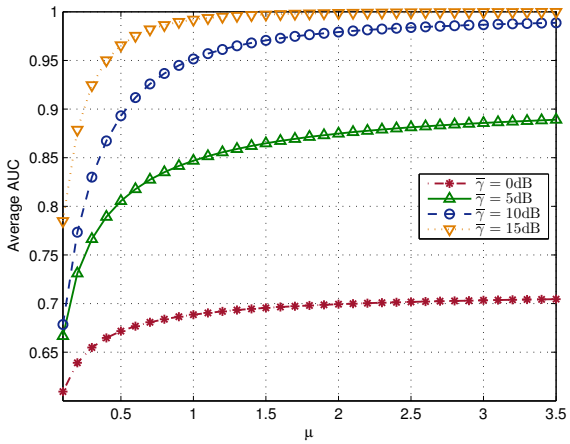

Fig. 6. Average AUC versus μ for $\eta-\mu$ fading with $u = 0.75$, $\eta = 0.3$, and different values of $\overline{\gamma}$.

noteworthy for its lower values. This also demonstrates that the effect of severe fading on the system performance is stronger as the average SNR increases.

Fig. 4 shows the AUC curves for the $\eta-\mu$ fading channel model for different η and μ values with $u = 3$ under Format I. It can be seen that the energy detector shows better detection capability for higher μ (with fixed η) due to the advantage of multipath effect. Meanwhile, the energy detector shows better performance for higher η ($0 < \eta \leq 1$ and with fixed μ) because the receiver receives more power through in-phase components. For example, for the case of $\overline{\gamma} = 10$dB and $\mu = 0.1$ (fixed), the $\overline{A}$ for $\eta = 0.5$ is nearly 1.6% higher than for $\eta = 0.25$. In the same context, when $\eta = 0.1$ (fixed), the $\overline{A}$ for $\mu = 0.5$ is 8.6% higher than for the case of $\mu = 0.25$. Fig. 4 illustrates the case in which $\eta \to 1$ ($\mu = 0.1$) and the case in which $\mu = 0.5$ ($\eta = 0.1$) coincides with that for Hoyt with $b = 0.82$, where b is the Hoyt parameter, or equivalently with that of Nakagami-q with $q^2 = 0.1$.

Finally, Figs. 5−6 depict the effect of the fading parameters on the sensing performance of energy detection based method over $\eta-\mu$ fading channels. Fig. 5 shows the behavior of $\overline{A}$ versus η curves for $u = 0.75$, $\mu = 0.5$, and different values of $\overline{\gamma}$. One can clearly notice that the value of $\overline{A}$ changes gradually at variations of η in the area $0 < \eta \leq 1$. Note that, since the distribution is symmetrical around $\eta = 1$, within $0 < \eta^{-1} \leq 1$ the energy detector shows better performance for lower η. In the same context, Fig. 6 demonstrates the behavior of $\overline{A}$ versus μ curves for $u = 0.75$, $\mu = 0.3$, and different values of $\overline{\gamma}$. It is clearly shown that the $\overline{A}$ is very sensitive as even slight variations of μ creates detrimental effects in $\overline{A}$.

V. Concluding Remarks

Exact analytic expressions are derived for the average AUC in energy detection based spectrum sensing over AWGN, $\kappa-\mu$, and $\eta-\mu$ fading channels. These expressions are represented in closed-form in terms of known generalized hypergeomteric functions and also account for fractional values of the involved time-bandwidth product. The offered results show that the detection capability for $\kappa-\mu$ fading increases when the ratio between the total power of the dominant components and the total power of the scattered waves increase and this also holds for the $\eta-\mu$ when more power is received due to the in-phase components. It is anticipated that the offered results will be useful in future analyses and design of cognitive radio systems.

Acknowledgment

This work was supported by the Finnish Funding Agency for Technology and Innovation (Tekes) under the project entitled "Energy-Efficient Wireless Networks and Connectivity of Devices-Systems (EWINE-S)", by the Academy of Finland under the projects No. 251138 Digitally-Enhanced RF for Cognitive Radio Devices and No. 284694 "Fundamentals of Ultra Dense 5G Networks with Application to Machine Type Communication" and by the UK Engineering and Physical Science Research Council (EPSRC).

References

[1] J. Mitola III, G. Q. Maguire Jr, "Cognitive radio: making software radios more personal," *IEEE Pers. Commun.*, vol. 6, no. 4, pp. 13−18, 1999.

[2] D. Čabrić, S. M. Mishra, and R. W. Brodersen, "Implementation issues in spectrum sensing for cognitive radios," *IEEE Conference on Signals, Systems and Computers*, pp. 772−776, 2004.

[3] S. Dikmese, P. C. Sofotasios, T. Ihalainen, M. Renfors, and M. Valkama, "Efficient Energy Detection Methods for Spectrum Sensing under Non-Flat Spectral Characteristics," *IEEE J. on Sel. Areas Commun.*, vol. 33, no. 5, pp. 755−770, May 2015.

[4] A. Bagheri, A. Shahini, and A. Shahzadi, "Analytical and learning-based spectrum sensing over channels with both fading and shadowing," *IEEE International Conference on Connected Vehicles and Expo (ICCVE)*, pp. 699−706, Dec. 2013.

[5] Sh. Tabatabaee, A. Bagheri , A. Shahini, and A. Shahzadi, "An analytical model for primary user emulation attacks in IEEE 802.22 networks," *IEEE International Conference on Connected Vehicles and Expo (ICCVE)*, pp. 693−698, Dec. 2013.

[6] P. C. Sofotasios, M. Valkama, T. A. Tsiftsis, Y. A. Brychkov, S. Freear, and G. K. Karagiannidis, "Analytic solutions to a Marcum Q-function-based integral and application in energy detection of unknown signals over multipath fading channels," in *in Proc. CROWNCOM '14*, Oulu, Finland, 2−4 June, 2014, pp. 260−265.

[7] H. Ding, W. Liu, X. Huang, and L. Zheng, "First path detection using rank test in IR UWB ranging with energy detection receiver under harsh environments," *IEEE Commun. Lett.*, vol. 17, no. 4, pp. 761−764, 2013.

[8] D. Zogas, G. K. Karagiannidis and S Kotsopoulos, "On the average output SNR in selection combining with three correlated branches over Nakagami−m fading channels," *IEEE Trans. Wireless Commun.*, vol. 3, no. 1, pp. 25−28, Jan. 2004.

[9] G. K Karagiannidis, D. Zogas, N.C Sagias, T. A. Tsiftsis, P. T. Mathiopoulos, "Multihop communications with fixed-gain relays over generalized fading channels," *IEEE GLOBECOM '04*, pp. 36−40.

[10] P. C. Sofotasios and S. Freear, "The $\kappa - \mu$/gamma Composite Fading Model," *IEEE ICWITS '10*, Honolulu, HI, USA, Aug. 2010.

[11] K. Ho-Van, P. C. Sofotasios, and S. Freear, "Underlay Cooperative Cognitive Networks with Imperfect Nakagami−m Fading Channel Information and Strict Transmit Power Constraint: Interference Statistics and Outage Probability Analysis," *IEEE/KICS Journal of Communications and Networks*, vol. 16, no. 1, pp. 10−17, Feb. 2014.

[12] D. Zogas and G. K. Karagiannidis, "Infinite-series representations associated with the bivariate Rician distribution and their applications," *IEEE Trans. Commun.*, vol. 53, no. 11, pp. 1790−1794, Nov. 2005.

[13] P. C. Sofotasios and S. Freear, "The $\alpha - \kappa - \mu$ Extreme Distribution: Characterizing Non Linear Severe Fading Conditions," *ATNAC '11*, Melbourne, Australia, Nov. 2011.

[14] D.S. Michalopoulos, G.K. Karagiannidis, T. A. Tsiftsis, and R. K. Mallik, "An optimized user selection method for cooperative diversity systems," *IEEE GLOBECOM '06*, pp. 1−6.

[15] P. C. Sofotasios, T. A. Tsiftsis, M. Ghogho, L. R. Wilhelmsson and M.Valkama, "The $\eta - \mu$/Inverse-Gaussian Distribution: A Novel Physical Multipath /Shadowing Fading Model," *IEEE ICC '13*, Budapest, Hungary, June 2013.

[16] Z Hadzi-Velkov, N. Zlatanov, G.K. Karagiannidis "On the second order statistics of the multihop Rayleigh fading channel," *IEEE Trans. Commun.*, vol. 57, no. 6, pp. 1815−1823, June 2009.

[17] P. C. Sofotasios, T. A. Tsiftsis, K. Ho-Van, S. Freear, L. R. Wilhelmsson, and M. Valkama, "The $\kappa - \mu$/Inverse-Gaussian Composite Statistical Distribution in RF and FSO Wireless Channels," *in IEEE VTC '13 - Fall*, Las Vegas, USA, pp. 1−5, Sep. 2013.

[18] S, Harput, P. C. Sofotasios, and S. Freear, "A Novel Composite Statistical Model For Ultrasound Applications," *Proc. IEEE IUS '11*, pp. 1−4, Orlando, FL, USA, 8−10 Oct. 2011.

[19] D. S Michalopoulos, A. S. Lioumpas, G. K. Karagiannidis and R. Schober "Selective cooperative relaying over time-varying channels," *IEEE Trans. Commun.*, vol. 58, no. 8, pp. 2402−2412, Aug. 2010.

[20] P. C. Sofotasios, M. Valkama, Yu. A. Brychkov, T. A. Tsiftsis, S. Freear and G. K. Karagiannidis, "Analytic Solutions to a Marcum $Q-$Function-Based Integral and Application in Energy Detection," *in CROWNCOM 14*, Oulu, Finland, pp. 260−265, June 2014.

[21] P. C. Sofotasios, T. A. Tsiftsis, Yu. A. Brychkov, S. Freear, M. Valkama, and G. K. Karagiannidis, "Analytic Expressions and Bounds for Special Functions and Applications in Communication Theory," *IEEE Trans. Inf. Theory*, vol. 60, no. 12, pp. 7798−7823, Dec. 2014.

[22] H. Urkowitz, "Energy detection of unknown deterministic signals," *Proc. IEEE*, vol. 55, no. 4, pp. 523−531, 1967.

[23] F. F. Digham, M.-S. Alouini, and M. K. Simon, "On the energy detection of unknown signals over fading channels," *IEEE Trans. Commun.*, vol. 55, no. 1, pp. 21−24, 2007.

[24] S. Atapattu, C. Tellambura, and H. Jiang, "Performance of an energy detector over channels with both multipath fading and shadowing," *IEEE Trans. Wireless Commun.*, vol. 9, no. 12, pp. 3662−3670, 2010.

[25] S. P. Herath, N. Rajatheva, and C. Tellambura, "Energy detection of unknown signals in fading and diversity reception," *IEEE Trans. Commun.*, vol. 59, no. 9, pp. 2443−2453, Sept. 2011.

[26] P. Sofotasios, E. Rebeiz, L. Zhang, T. A. Tsiftsis, D. Čabrić, and S. Freear, "Energy detection based spectrum sensing over $\kappa-\mu$ and extreme $\kappa-\mu$ fading channels," *IEEE Trans. Veh. Technol.*, vol. 62, no. 3, pp. 1031−1040, Mar. 2013.

[27] P. C. Sofotasios, M. K. Fikadu, Kh. Ho-Van, and M. Valkama, "Energy detection sensing of unknown signals over Weibull fading channels," *IEEE ATC '13*, pp. 414−419, Oct. 2013.

[28] A. Shahini, A. Bagheri, and A. Shahzadi, "A unified approach to performance analysis of energy detection with diversity receivers over Nakagami-m fading channels," *IEEE International Conference on Connected Vehicles and Expo (ICCVE)*, pp. 707−712, Dec. 2013.

[29] A. Bagheri, and A. Shahzadi, "Another look at performance analysis of energy detector with multichannel reception in Nakagami-m fading channels," *Wireless Pers. Commun.*, vol. 79, no. 1, pp. 527−544, 2014.

[30] S. Atapattu, C. Tellambura, and H. Jiang, "Analysis of area under the ROC curve of energy detection," *IEEE Trans. Wireless Commun.*, vol. 9, no. 3, pp. 1216−1225, 2010.

[31] A. Bagheri, P. C. Sofotasios, T. A. Tsiftsis, A. Shahzadi, and M. Valkama, "Spectrum Sensing in Generalized Multipath Fading Conditions Using Square-Law Combining," *In Proc. IEEE ICC '15*, London, UK. June 2015.

[32] P. C. Sofotasios, M. K. Fikadu, K. Ho-Van, M. Valkama, and G. K. Karagiannidis, "The area under a receiver operating characteristic curve over enriched multipath fading conditions," *in IEEE Globecom '14*, Austin, TX, USA, pp. 3090−3095, Dec. 2014.

[33] A. Bagheri, P. C. Sofotasios, T. A. Tsiftsis, A. Shahzadi, and M. Valkama, "AUC Study of Energy Detection Based Spectrum Sensing over $\eta-\mu$ and $\alpha-\mu$ Fading Channels," *In Proc. IEEE ICC '15*, London, UK. June 2015.

[34] S. Atapattu, C. Tellambura, and H. Jiang, "Performance of energy detection: A complementary AUC approach," in *IEEE Global Telecommunications Conference (GLOBECOM)*, pp. 1−5, Dec. 2010.

[35] S. Atapattu, C. Tellambura, and H. Jiang, "MGF based analysis of area under the ROC curve in energy detection," *IEEE Commun. Lett.*, vol. 15, no. 12, pp. 1301−1303, Dec. 2011.

[36] S. Alam, O. Odejide, O. Olabiyi, and A. Annamalai, "Further results on area under the ROC curve of energy detectors over generalized fading channels," in *Proceedings* 34^{th} *IEEE Sarnoff Symposium*, pp. 1−6, May 2011.

[37] O. Olabiyi, S. Alam, O. Odejide, and A. Annamalai, "Efficient evaluation of area under the ROC curve of energy detectors over fading channels," in *the* 14^{th} *ACM International Conference on Modeling, Analysis and Simulation of Wireless and Mobile Systems (MSWiM)* , Miami Beach, FL, USA, pp. 261−264, Oct. 2011.

[38] M. D. Yacoub, "The $\kappa-\mu$ distribution and the $\eta-\mu$ distribution," *IEEE Antennas Propag. Mag.*, vol. 49, no. 1, pp. 68−81, 2007.

[39] J. I. Marcum, "Table of Q functions," Rand Croporation, Santa Monica, CA, U.S. Air Force Project RAND Research Memorandum M-339, ASTIA Document AD 1165451, Jan. 1950.

[40] I. S. Gradshteyn and I. M. Ryzhik, *Table of integrals, series, and products*, in 7^{th} ed. Academic, New York, 2007.

[41] M. Abramowitz, and I. A. Stegun, *Handbook of mathematical functions with formulas, graphs, and mathematical tables*, New York: Dover, 1974.

[42] H. M. Srivastava and H. L. Manocha, *A Treatise on Generating Functions*, Halsted Press, John Wiley & Sons, New York, 1984.

[43] Wolfram, *The wolfram functions site*. [Online]. Available: *http://functions.wolfram.com*.

[44] J. Choi, A. Hasanov, and M. Turaev, "Decomposition formulas and integral representations for some Exton hypergeometric functions," *Journal of the Chungcheong Math. Society*, vol. 24, no. 4, pp. 745−758, 2011.